Signal feature recognition based on lightwave neuromorphic signal processing

Mable P. Fok,[1,*] Hannah Deming,[1] Mitchell Nahmias,[1] Nicole Rafidi,[1] David Rosenbluth,[2] Alexander Tait,[1] Yue Tian,[1] and Paul R. Prucnal[1]

[1]*Lightwave Communication Research Laboratory, Department of Electrical Engineering, Princeton University, Princeton, New Jersey 08544, USA*

[2]*Lockheed Martin Advanced Technologies Laboratory, Cherry Hill, New Jersey 08002, USA*

**Corresponding author: mfok@princeton.edu*

Received September 1, 2010; revised November 10, 2010; accepted November 12, 2010; posted November 22, 2010 (Doc. ID 134383); published December 16, 2010

We developed a hybrid analog/digital lightwave neuromorphic processing device that effectively performs signal feature recognition. The approach, which mimics the neurons in a crayfish responsible for the escape response mechanism, provides a fast and accurate reaction to its inputs. The analog processing portion of the device uses the integration characteristic of an electro-absorption modulator, while the digital processing portion employ optical thresholding in a highly Ge-doped nonlinear loop mirror. The device can be configured to respond to different sets of input patterns by simply varying the weights and delays of the inputs. We experimentally demonstrated the use of the proposed lightwave neuromorphic signal processing device for recognizing specific input patterns.

OCIS codes: 070.4340, 320.7085, 200.4700.

Neuromorphic engineering provides a wide range of practical computing and signal processing tools by exploiting the biophysics of neuronal computation algorithms. Existing technologies include analog very-large-scale integration front-end sensor circuits that replicate the capabilities of the retina and the cochlea [1]. To meet the requirements of real-time signal processing, lightwave neuromorphic signal processing [2,3] can be utilized to provide the high-speed and low-latency performance that is characteristic of photonic technology. Lightwave neuromorphic signal processing incorporates hybrid analog and digital processing techniques that take advantage of both the bandwidth efficiency of analog processing and the low-noise characteristics of digital processing. Previous work demonstrated a photonic pulse processing device based on the integrate-and-fire neuron model [3] for the optical realization of a spiking neuron.

In this Letter, we propose and demonstrate a device for signal feature recognition based on the escape response neuron model of a crayfish [4]. Crayfish escape from danger by means of a rapid escape response behavior. The corresponding neural circuit is configured to respond to appropriately sudden stimuli. Since this corresponds to a life-or-death decision for the crayfish, it must be executed quickly and accurately. A potential application of the escape response circuit based on lightwave neuromorphic signal processing could be for pilot ejection from military aircraft. Our device, which mimics the crayfish circuit using photonic technology, is sufficiently fast to be applied to defense applications in which critical decisions need to be made quickly while minimizing the probability of false alarm.

Our device exploits fast (subnanosecond) signal integration in electro-absorption modulators (EAM) and ultrafast (picosecond) optical thresholding in highly Ge-doped nonlinear loop mirrors (Ge-NOLM). The basic model consists of two cascaded integrators and one optical thresholder. The first integrator is configured to respond to a set of signals with specific features, while the second integrator further selects a subset of the signal from a set determined by a weighting and delay configuration and responds only when the input stimuli and the spike from the first integrator arrive within a very short time interval.

Figure 1 illustrates the (a) crayfish escape neuron model and (b) optical realization of the escape response for signal feature recognition. As shown in Fig. 1(a), signals from the receptors (R) are directed to the first stage of neurons—the sensory inputs (SI). Each of the SI is configured to respond to specific stimuli at the receptors. The SI integrate the stimuli and generate spikes when the inputs match the default feature. The spikes are then launched into the second stage of the neural circuit—the lateral giant (LG). The LG integrates the spikes from the first stage and one of the receptor signals. The neuron responds only when the signals are sufficiently close temporally and strong enough to induce a spike—an abrupt stimulus.

In the analog optical model shown in Fig. 1(b), inputs a, b, and c are weighted and delayed such that the first

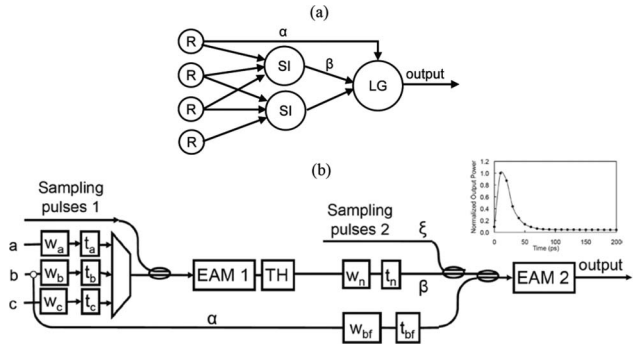

Fig. 1. (a) Schematic illustration of the crayfish tail-flip escape response. R, receptors; SI, sensory inputs; LG, lateral giant. (b) Schematic illustration of the optical implementation of the escape response. w, weight; t, delay; EAM, electro-absorption modulator; TH, optical thresholder. Inset, measured recovery temporal profile of cross-absorption modulation in EAM.

EAM (CIP 10G-PS-EAM-1550) integrator (EAM 1) is configured to spike for inputs with specific features. A train of sampling pulses is launched together with the inputs to provide a pulsed source for the EAM to spike. The spiking behavior is based on cross-absorption modulation (XAM) [5] in an EAM. That is, when the integrated input power is large enough for XAM to occur, the sampling pulses within the integration window are passed through the EAM; otherwise they are absorbed. The spike output is then thresholded at the Ge-NOLM [6] such that the output spikes are of similar height, and the undesired weak spikes are removed. The thresholded output and part of input b are launched into the second integrator (CIP 10G-LR-EAM-1550) as the input control through path β and α, respectively. Sampling pulses are launched to the integrator through path ξ as a spiking source. Through weighting and delaying of the inputs, spikes by the second integrator occur only for inputs with the desired features. The selection of the desired features can be reconfigured simply by adjusting the weights and delays of the inputs.

The integration of a signal at the EAM is based on the finite XAM recovery time of a negatively biased EAM. The inset in Fig. 1(b) shows the recovery time of an EAM. Maximum transmittance is obtained when the sampling pulse is very close to the input control pulse, and the transmittance decreases gradually as the time delay increases. Therefore, by placing multiple control pulses within the recovery interval, the EAM integrates them. Figure 2(a) shows the input control signal consisting of one, two, or three pulses that are within the integration window. After integration at the EAM, the sampling pulses representing the integrated output are shown in Fig. 2(b) with the superimposed temporal profiles shown in the insets. The EAM is adjusted to spike when the input has two or more pulses occurring within the integration time. To equalize the heights of the output and remove the unwanted weak pulses, a Ge-NOLM thresholder is used. Figure 3 shows the experimental measurement of the thresholder transfer function (filled squares), as well as the simulated transfer function using the VPIphotonics simulation tool (triangles).

In this signal feature recognizer experiment, there are three inputs, a, b, and c. The recognition circuit detects input patterns of abc and ab- having specific time intervals between the inputs as we configured, as shown in Fig. 4. Figure 4, part (i), shows five different input combinations, where input a is designed to have the largest

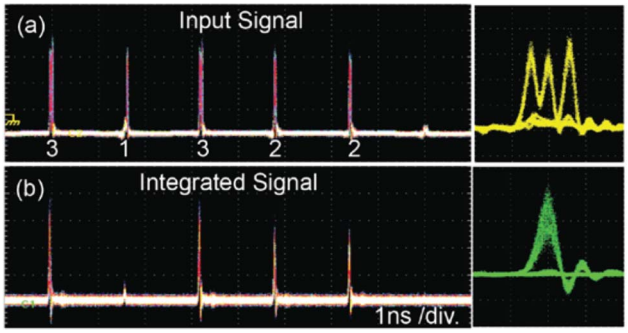

Fig. 2. (Color online) (a) Input to EAM. (b) Output sampling pulses of EAM. Insets, superimposed output temporal profiles.

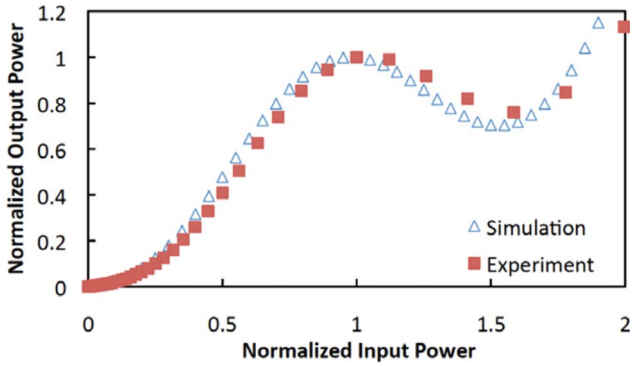

Fig. 3. (Color online) Experimental (solid squares) and simulation (open triangles) results of the optical thresholder transfer function.

weight, while input b has the smallest weight. The separation of each set of inputs is sufficiently large that they do not affect each other's integration performance. Five sampling pulses are used for each set of inputs, as shown in Fig. 4, part (ii). With the use of multiple sampling pulses, high temporal resolution of the integration, as well as differing spike patterns for the second stage of integrator, can be obtained. The input pulses change the transmittance of the EAM 1 as shown by the curves in Fig. 4, part (iii); thus the amplitude of the sampling pulses (shaded pulses) at the EAM 1 output also changed. The output spikes from EAM 1 are then thresholded at the level indicated by the dotted line. The spikes are now of similar amplitude and the undesired weak spikes are removed [Fig. 4, part (iv)]. Different spike patterns are obtained for different inputs. In this experiment, we identify patterns abc and ab-. Here, we use the EAM 1 output as the sampling pulse, which also helps eliminate

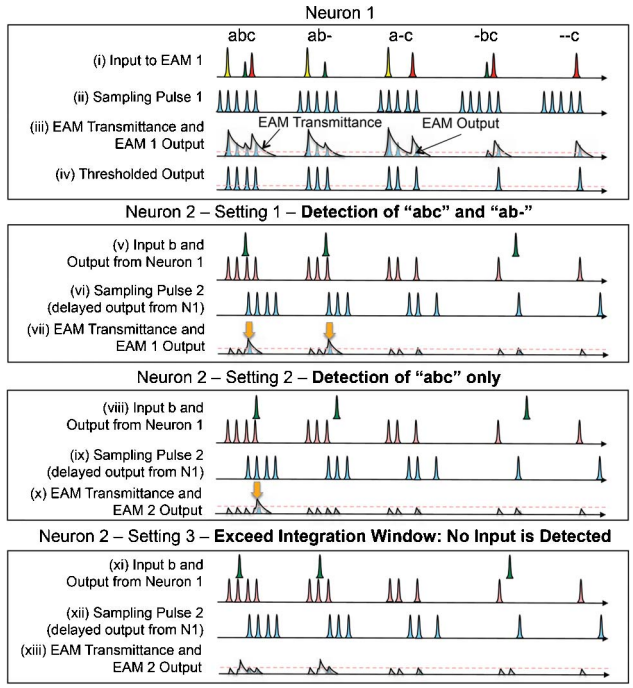

Fig. 4. (Color online) Schematic illustration of configuring the pattern recognition. (i)–(iv) First integrator and thresholder. (v)–(vii) Setting 1, detection of abc and ab-. (viii)–(x) Setting 2, detection of abc only. (xi)–(xiii) Setting 3, exceed integration window—no input is detected.

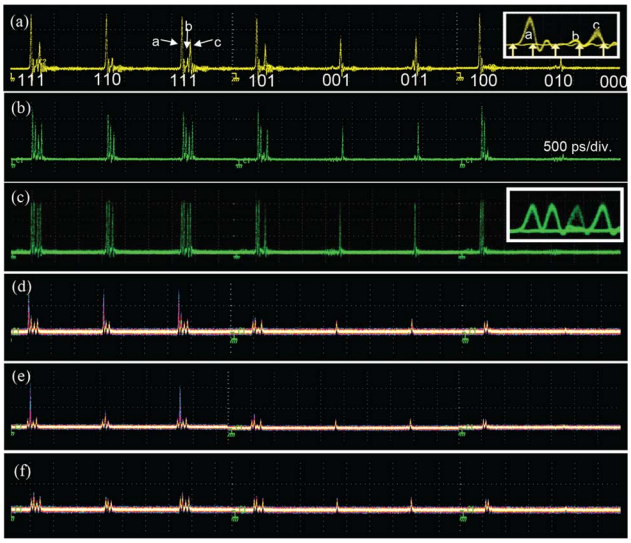

Fig. 5. (Color online) Experimental results. (a) Optical inputs to EAM 1; (b) different spike patterns resulted from the first integrator; (c) thresholded output; (d) output spikes from EAM 2, recognizing pattern *abc* and *ab*-; (e) output spike from EAM 2, recognizing pattern *abc* only; (f) output from EAM 2, none of the input is recognized.

undesired patterns; i.e., input *a* is absent. The EAM 1 output is launched into the second integrator as sampling pulses, while a duplicated, delayed, and weighted copy is combined with input *b* and used as the control for the second integrator [Fig. 4, part (v)]. By adjusting the relative temporal delay between the input *b* and the inputs to the EAM 2, different input features are recognized, as shown in Figs. 4, parts (v)–(xiii).

Figure 5 shows the experimental measurements of the signal feature recognizer. In the experiment, the input signal has an average power of ~2.5 dBm. Figure 5(a) shows all eight combinations of the three inputs with specific weights and delays. We use "1" to represent the presence of input, while "0" means there is no input. Superimposed temporal profile of the input signal is shown in the inset of Fig. 5(a). Sampling pulses with power of −9 dBm and separation of ~25 ps are used, as indicated by the arrows. The input signals are integrated, and the transmittance of the EAM 1 is represented by the spike pattern at the output [Fig. 5(b)]. A Ge-NOLM is used to threshold the output of EAM 1 [Fig. 5(c)]. The inset shows the superimposed temporal profile of the thresholded output. Four-wave mixing in a 35 cm bismuth-oxide nonlinear fiber is used [7] to duplicate the thresholded output. Two copies at different wavelengths are obtained, one as the sampling pulses and one as the input to the EAM 2. The sampling pulses are at −1.25 dBm, while the input signal to the EAM 2 is at 4.7 dBm. When the output spikes from the first neuron arrive at the second integrator slightly after input *b*, i.e., within the integration interval, the second integrator will spike. By adjusting the time delay of the inputs to the EAM 2, the pattern recognizer identifies patterns *abc* and *ab*- [Fig. 5(d)] or just *abc* [Fig. 5(e)]. However, when the spikes from the first neuron arrive too late, i.e., exceed the integration time, the second integrator will not spike [Fig. 5(f)]. These examples indicate that the signal feature recognizer is performing correctly and is reconfigurable through time delay adjustment.

We experimentally demonstrate signal feature recognition based on the principle of the escape response of a crayfish. The approach exploits the finite recovery time of cross-absorption modulation in EAM to implement signal integration, while thresholding is implemented using a Ge-doped fiber-based NOLM. By adjusting the weights and delays of the inputs, the feature recognizer can be configured to identify different signal features. This hybrid analog/digital signal processing technique allows a fast and accurate response to the inputs.

The authors gratefully acknowledge the generous support of the Lockheed Martin Advanced Technology Laboratory through their IRAD program, as well as the Lockheed Martin Corporation through their Corporate University Research Program. The authors also acknowledge the support of the National Science Foundation (NSF) MIRTHE Center at Princeton University.

References

1. C. Koch and H. Li, *Vision Chips: Implementing Vision Algorithms With Analog VLSI Circuits* (IEEE Computer Science Press, 1994).
2. M. P. Fok, D. Rosenbluth, K. Kravtsov, and P. R. Prucnal, IEEE Signal. Process. Mag. **27**, 158 (2010).
3. D. Rosenbluth, K. Kravtsov, M. P. Fok, and P. R. Prucnal, Opt. Express **17**, 22767 (2009).
4. P. J. Simmons and D. Young, *Nerve Cells and Animal Behaviour* (Cambridge U. Press, 1999).
5. N. Edagawa, M. Suzuki, and S. Yamamoto, IEICE Transactions on Electronics **E81-C**, 1251 (1998).
6. K. Kravtsov, P. R. Prucnal, and M. M. Bubnov, Opt. Express **15**, 13114 (2007).
7. M. P. Fok and C. Shu, J. Lightwave Technol. **27**, 2953 (2009).